European Journal of Pharmaceutics and Biopharmaceutics 125 (2018) 21–27

Contents lists available at ScienceDirect

European Journal of Pharmaceutics and Biopharmaceutics

journal homepage: www.elsevier.com/locate/ejpb

Research paper

In vivo release of peptide-loaded PLGA microspheres assessed through deconvolution coupled with mechanistic approach

Ivana Tomic[a,b,*], Martin Mueller-Zsigmondy[a], Ana Vidis-Millward[a], Jean-Michel Cardot[b]

[a] Novartis Pharma AG, Technical Research and Development, CH-4002 Basel, Switzerland
[b] University of Auvergne, Department of Biopharmacy, EA 4678, 63001 Clermont-Ferrand, France

ARTICLE INFO

Keywords:
PLGA microspheres
Drug release
Numerical deconvolution
Weibull function
Peppas power model

ABSTRACT

In this study, a reevaluation of the *in vivo* release phases from long-release PLGA-based microspheres is presented, leading to a better characterization of the plasma concentrations/time profile. Microspheres were designed for intramuscular injection releasing a cyclic somatostatin analog over 70 days. Clinical study was performed in 64 healthy subjects receiving a subcutaneous dose of an immediate release solution as reference formulation and an intramuscular injection of microspheres as test formulation. The *in vivo* input curve was obtained by numerical deconvolution.

Results showed that double Weibull function could not fit correctly the tri-phasic (burst, lag, and erosion) *in vivo* input profile typical for PLGA-based formulations, due to a change in the drug release trend in the terminal phase. Triple Weibull showed a significant improvement in the curve fitting, each term being assigned to one of the following phases: initial (burst/lag), erosion, and terminal phase of drug release. The existence of the additional terminal phase was confirmed by a mechanistic approach as well, which denoted that this phase was, most probably, a consequence of the release mechanism change from erosion to diffusion controlled. The same model demonstrated that the burst release was as well influenced by the polymer swelling, while currently existing theories state that the burst phase is mainly determined by the dissolution of immediately available drug substance and diffusion through surface related pores.

1. Introduction

In vitro-In vivo correlation (IVIVC) is defined by health authorities as a mathematical relationship between the *in vitro* dissolution and *in vivo* properties of a drug product [1,2]. It is a useful tool in the drug product development as it can support formulation optimization, dissolution specification setting, or it can be used as a surrogate for bioequivalence (BE) studies.

In order to obtain the *in vitro* data, a biorelevant dissolution method, reflecting the *in vivo* release process, should be developed for the tested drug product. On the other hand, the *in vivo* input (release/dissolution/permeation) cannot be measured directly from formulated drugs. It should be generated from the plasma concentration data which are commonly available after the administration of a drug product [3].

The process of deriving the *in vivo* input from the plasma concentration data is called deconvolution [4]. The plasma concentration versus time profile is a representation of the dissolution process, permeation (drug input into the systemic circulation), and the disposition (distribution and elimination). The role of the deconvolution process is characterization of the drug input rate. For this purpose, it is necessary to define the drug disposition by the use of some unit impulse response (UIR), such as an intravenous dose or an immediate release (IR) solution. Two main groups of deconvolution techniques exist: (i) model-dependent based on an assumption of a drug disposition model (illustrated by Wagner-Nelson [5] and Loo-Riegelman [6]) and (ii) model-independent based on numerical algorithms [7,8] (without limitation considering the disposition). The advantage of the numerical deconvolution is that it can separate the *in vivo* dissolution from the permeation process in case the UIR describes the permeation as well [4].

A special case of the numerical deconvolution is a deconvolution-through-convolution (DTC) [9–12]. This method allows not only generation, but also modeling of the *in vivo* input function and subsequent back calculation of the plasma concentrations by convolution. The calculated plasma concentrations are then compared to the observed data, assessing in such a way the internal predictability of the deconvolution method. In the DTC procedure, modeling of the input curve and subsequent convolution are based on the same distribution function. A general empirical equation, first described by Weibull [13] then

* Corresponding author at: Novartis Pharma AG, TRD, Physic Garden 3 – 3.14.49, CH-4002 Basel, Switzerland.
E-mail address: ivana.tomic@novartis.com (I. Tomic).

https://doi.org/10.1016/j.ejpb.2017.12.007
Received 11 April 2017; Received in revised form 23 November 2017; Accepted 15 December 2017
Available online 19 December 2017
0939-6411/

adapted by Langenbucher [14] to the dissolution process, is the most frequently used for this purpose. It represents a flexible function that can be successfully applied to various kinds of dissolution curves. Nevertheless, Costa and Lobo [15] highlight in their work some disadvantages of this function as: (i) the lack of a kinetic base (characterization of the curve is limited to description) and (ii) the lack of relation between its parameters and dissolution process. Therefore, a complete characterization of the *in vivo* input profile, which is an essential part of the IVIVC development, still remains very challenging. This is particularly the case with injectable long-release delivery systems that tend to demonstrate very complex drug release patterns.

It was demonstrated, for example, that injectable long-release delivery systems based on poly(lactide-*co*-glycolide) acid (PLGA) can show a sustained drug release controlled by diffusion, polymer erosion, or a combination of both mechanisms [16–18]. As a result, different phases can be distinguished during the *in vivo* release process, such as: burst, lag, and erosion. Consequently, the plasma concentrations/time profile can show more than one peak.

The objective of this paper is to provide an example of using a special case of the numerical deconvolution process (DTC) for describing the multiphasic *in vivo* input curve and discernment of release phases for peptide-loaded PLGA-based microspheres after intramuscular injection in humans. The DTC method described by Langenbucher was selected as it allows generation of the *in vivo* input curve (by deconvolution) and its separation into different release phases (by an integrated mathematical function). The goal was to describe each phase of the drug release (burst, lag, erosion) separately by the use of Weibull function. The curve shape during various release phases was described by the Weibull shape factor, while the separation into phases was confirmed by a mechanistic model (The Peppas' power law [19]).

Based on this approach, different phases appearing during the release process from PLGA-based microspheres in human subjects were reevaluated and related to the corresponding release mechanism. The complete characterization of the *in vivo* input curve performed in such way can further allow easier and faster simulation of the release processes under *in vitro* conditions and, thus, establishment of a relationship between the *in vitro* and *in vivo* data.

2. Material and methods

2.1. Material

A cyclic somatostatin analog (MW ≈ 1 kDa) in a form of salt, was encapsulated in microspheres of 50% branched PLGA (MW ≈ 52 kDa) and 50% linear PLGA (MW ≈ 12 kDa). Both polymers were a mixture of 50% lactic acid and 50% glycolic acid. Peptide and branched polymer were from Novartis Pharma AG (Basel, CH), and linear polymer was from Boehringer Ingelheim (Ingelheim, DE). Poly(vinyl alcohol) (PVA) was obtained from Sigma (St. Louis, MO). Methylene chloride, disodium hydrogen phosphate, potassium dihydrogen phosphate, and water for injection were obtained from Merck (Darmstadt, DE).

2.2. Preparation of microspheres (MS)

A multiple emulsion technique was used for preparation of peptide-loaded PLGA microspheres. Briefly, a mixture of branched and linear PLGA was dissolved in methylene chloride and filtered. The peptide was added to the prepared polymer solution and obtained dispersion was then injected in aqueous solution of PVA. In order to obtain solid microspheres, prepared emulsion was mixed at a higher temperature to allow the evaporation of methylene chloride. The solidified microspheres were filtered and washed by water for injection and then dried in a vacuum dryer.

2.3. Characterization of the microspheres

2.3.1. Determination of initial drug loading

Approximately 20 mg peptide-loaded microspheres were dissolved in 10 mL of acetonitrile:methanol (3:2) mixture. The samples were centrifuged at 3500 rpm for 10 min, and the supernatant was analyzed using the HPLC system.

2.3.2. Differential scanning calorimeter (DSC)

The samples were analyzed using TA Instruments 2920 DSC. The samples were heated up to 80 °C and cooled down to 5 °C at a rate of 10 °C/min; the second cycle was used to determine the glass transition temperature (Tg). The samples were analyzed in aluminum pans with pinhole lids.

2.3.3. Particle size analysis

The particle size of the microspheres was determined using a laser particle size analyzer (Sympatec HELOS, Sympatec GmbH, Germany). One hundred milligrams of microspheres were suspended in 6 mL of distilled water and subjected to vortex mixing for 10 sec before the analysis.

2.4. Clinical study design

The study was designed with the aim to assess pharmacokinetics and safety of long-release microspheres (LR MS) applied intramuscularly (i.m.) vs subcutaneous (s.c.) administration of an IR solution. It was a crossover design study conducted in male healthy volunteers. In total, 64 subjects completed the study and each subject received 1 mL of an IR solution containing 300 µg of the peptide, as s.c. administration in the abdominal wall. After a 14-day wash out period, subjects received 2 mL of the LR MS suspension containing 60 mg of the peptide. The i.m. injection was administered into the left or right gluteal muscle. Both, s.c. and i.m. doses were injected at approximately 8:00 am following an overnight fast of at least 8 h. No food was permitted until at least 4 h after the administrations. Both doses (s.c. 300 µg and i.m. 60 mg) were therapeutic, where the s.c. dose was developed as a solution for twice daily injection and i.m. was a depot formulation designed as a monthly injection.

Blood samples were taken from a forearm vein after s.c. injection at hours 0.25, 0.5, 1, 2, 4, 6, 8, 10, 12, 24, 48, 72, 96, 120, and 144. For the i.m. injection, one sample was taken pre-dose, then post-dose at hours 0.5, 1, 2, 4, 6, 8, 10, 12; and days 1, 2, 4, 6, 8, 10, 12, 14, 16, 18, 20, 22, 24, 26, 28, 35, 42, 49, 56, 63, and 70. The samples were centrifuged immediately. The plasma samples were kept frozen at ≤ −18 °C until analysis. The peptide plasma concentrations were then measured using a validated radio-immunoassay (RIA).

The study was conducted according to the ethical principles of the Declaration of Helsinki. The study protocol and all amendments were reviewed by the Independent Ethics Committee (IEC)/Institutional Review Board (IRB)/Research Ethics Board (REB). Informed consent was obtained from each subject in writing before conducting any study-specific procedures.

2.5. Deconvolution procedure

All calculations were performed on individual and mean profiles and obtained results were similar. Use of mean profile in the characterization of the *in vivo* input profile and establishment of an IVIVC was already discussed by Cardot et al. [20]. In order to simplify the present manuscript mean profiles are displayed.

2.5.1. Pharmacokinetics of immediate release subcutaneous injection – compartmental modeling

The data obtained after an IR s.c. injection, corresponding to the UIR, were used to determine the disposition kinetics of the peptide.

Fitting was performed using Phoenix WinNonlin, version 6.4 (Certara USA Inc, Princeton, NJ).

2.5.2. Deconvolution for long release intramuscular injection

Deconvolution was then performed on the data obtained after i.m. injection of LR MS in order to calculate the *in vivo* input profile of the peptide-loaded PLGA microspheres.

Numerical deconvolution is a non-compartmental method based on numerical algorithms. Segments of the response C_p are calculated as the sum of the input r in combination with segments of a weighting function C_δ, as represented by Eq. (1):

$$C_{p_{t_n}} = r_{t_n} * C_{\delta_{t_n}} \quad (1)$$

where: C_p represents the plasma drug concentration after the LR MS dose, C_δ is the plasma drug concentration after an UIR, r is the *in vivo* input rate and * is the convolution operator [2].

As the input function r is the unknown value, the inverse operation of deconvolution is performed using Eq. (2):

$$r_{t_n} = C_{p_{t_n}} // C_{\delta_{t_n}} \quad (2)$$

where // denotes deconvolution.

DTC (Deconvolution-through-convolution) method was described in details by Langenbucher [9–12]. It is based on the point-area approach using a staircase function; which is presented as a finite set of rectangular pulses of defined duration and intensity. The plasma drug concentration from the IR and LR MS formulations were used in the deconvolution process for calculation of the *in vivo* dissolution profile based on a prescribed function. Using the same function, the convolution step was then performed giving a predicted plasma concentration for the LR MS, which can be compared to the observed data, estimating a goodness of the chosen function.

The computation was performed in the Excel worksheet generated by Langenbucher [10].

Any model, such as zero or first order, could be used as cumulative input function in the Langenbucher approach. However, the most commonly used function in the deconvolution/convolution process is Weibull distribution, as it represents a descriptive function with high degree of flexibility, and it is defined by Eq. (3):

$$X_t = F_{\max}\left[1 - e^{-(t/\alpha)^\beta}\right] \quad (3)$$

where: X_t is the percentage of drug released at time t, F_{max} denotes max % released; α is the scale factor, β describes the shape of the curve as parabolic (β < 1), exponential (β = 1), or sigmoidal (β > 1) [11].

Fitting of the Weibull function was done by the Excel's Solver tool, GRG Nonlinear method [21].

Parameters of the function were modified, while minimizing the sum of the squared differences (SSQ) between observed and calculated plasma concentration values.

2.6. Statistical analysis

Goodness of fit of the tested function was estimated based on the Akaike Information Criterion (AIC), allowing the choice of the best fitting model and penalizing over-parametrization at the same time. This factor takes into account the residual SSQ between observed and predicted values as well as the number of time points and parameters.

2.7. Predictability

Percent prediction error (% PE) between observed and back-calculated pharmacokinetic (PK) parameters was then calculated using Eq. (4) to assess the internal predictability:

$$\%PE = |(Observedvalue - Predictedvalue)/Observedvalue| * 100 \quad (4)$$

An acceptance criterion for % PE is 15% or less for individual PK values and 10% or less for the average of PK values [1].

The predictability evaluation is an integral part of the Langenbucher's method as it performs deconvolution through convolution. Taking into consideration that convolution is calculated based on the deconvoluted *in vivo* input curve, it is expected that the % PE has a value of 0%.

2.8. Modeling of drug release from long release microspheres

Peppas [19] derived a simple, semi-empirical model (The power law) that relates the drug release to the time by the following equation:

$$\frac{X_t}{X_{inf}} = Kt^n \quad (5)$$

where: K is the release rate constant; n is the release exponent, indicator of the drug release mechanism. For spherical swellable controlled release systems, the release exponent $n \leq 0.43$ corresponds to Fickian diffusion, $0.43 < n < 0.85$ to anomalous (non-Fickian) transport, $n = 0.85$ to Case-II transport defined by polymer swelling and drug release controlled by relaxation and diffusion, and $n > 0.85$ to Super Case-II transport [19,22].

3. Results and discussion

3.1. Microspheres characteristics and glass transition temperature

The peptide loading was 25% (w/w). The particle size analyses showed a unimodal distribution with a mean diameter of about 40 µm. The glass transition temperature of the microspheres was determined to be 42 °C in dry state and below 30 °C in wet state (in distilled water).

3.2. Plasma concentrations after the subcutaneous and intramuscular application

The data obtained after administration of the IR solution as s.c. injection were analyzed using WinNonLin module in order to determine the disposition kinetics. Based on the AIC value, the best fitting model was the two-compartment with first-order input. The observed and fitted mean data are shown in Fig. 1 in log-linear scale.

The macro and micro rate constants are presented in Table 1.

Where: A and B are the macro coefficients; α and β are the hybrid macro rate constants of the distribution and elimination phases, respectively; k_{01}, k_{12}, k_{21}, and k_{el} are micro rate constants corresponding to the absorption, distribution (first to second compartment and vice versa), and elimination phase, respectively; and T_{max} is the time needed for maximal concentration to be achieved after the injection.

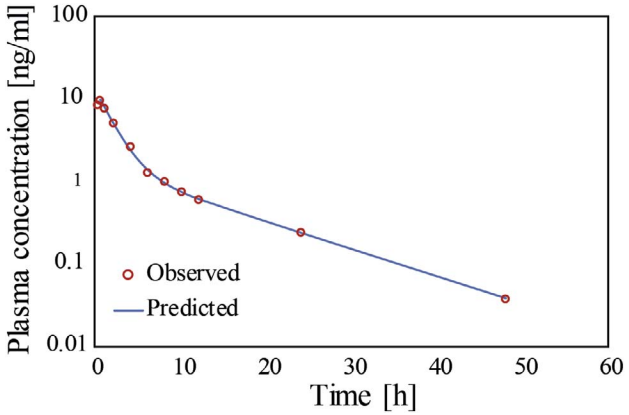

Fig. 1. Observed (◯) and predicted (——) plasma concentration after s.c. injection of the immediate release solution following two-compartment model, log-linear scale.

Table 1
PK parameters after the s.c. injection of peptide solution.

Parameter	A (ng/ml)	B (ng/ml)	α (h^{-1})	β (h^{-1})	k_{01} (h^{-1})	k_{el} (h^{-1})	k_{12} (h^{-1})	k_{21} (h^{-1})	AUC (ng h/ml)	T_{max} (h)
	10.7	1.4	0.5	0.1	8.3	0.3	0.2	0.1	37.7	0.4

Table 2 shows PK parameters obtained after the i.m. administration of LR MS formulation. Data were estimated by the Non-Compartmental Analyses (NCA) in WinNonLin module. $AUC_{0–48h}$, AUC_{last}, and AUC_{inf} are Area Under the Curve up to day 2 (covering burst phase), up to the last sampling point, and infinity, respectively. C_{max1} and C_{max2} correspond to the maximal concentrations during the burst and erosion phases, respectively. T_{max1} and T_{max2} represent the time needed for attaining the C_{max1} and C_{max2}, respectively.

Disposition function was obtained after the s.c. administration while the studied LR microspheres were applied intramuscularly. The absorption kinetic rates could differ for the two routes of administration due to the differences in physiology (*e.g.* vascularity). Nevertheless, as the peptide release from the LR formulation lasts for several weeks, any difference in the permeation rate from the injection site into systemic circulation is considered to be irrelevant. T_{max} after the s.c. injection was 0.4 h (see Table 1) indicating a very fast permeation through the tissue barriers; therefore, it can be assumed that the s.c. injection describes mainly the disposition and elimination. T_{max1} after the i.m. injection of microspheres was 24 h, which is significantly superior to T_{max} of the s.c. injection. This finding suggests that the appearance of the peptide in the systemic circulation after the i.m. injection is governed by the release from microspheres. Consequently, any potential difference in the permeation process compared to s.c. administration would not influence the final PK profile of LR MS, as the peptide release is the rate limiting step. Taking this into consideration, it is assumed that the solution administered as s.c. injection can be used as UIR in the deconvolution process.

The plasma concentrations/time profile after the i.m. injection of microspheres is shown in Fig. 2.

LR MS exhibited complex release kinetics, probably due to a short half-life of the peptide (2.3 h) in combination with the sustained release characteristics imposed by the technology of PLGA microspheres [23]. As shown in Fig. 2, plasma concentrations/time profile of the peptide follows a tri-phasic pattern: (i) initial peak at around 24 h corresponded to a burst phase, (ii) a decrease in concentration, defined as a "lag phase" (plateau at 48–144 h), and (iii) the onset of an erosion phase leading to an increase in concentration attaining a second peak around 500 h and followed by a decline of plasma concentration up to 1680 h. The drug release mechanism, responsible for such complex plasma concentrations/time profile typical for PLGA microspheres, was extensively studied [24–27]. Despite numerous studies already published in the literature, it is still very challenging to determine the true release mechanism, which depends on various factors (*e.g.* molecular weight of the polymer, drug substance properties, physiological environment, etc.) [28]. According to the currently existing theories, the burst phase depicts release of immediately available peptide at the surface of microspheres and initially existing pores; the lag phase represents time needed for polymer chains to start swelling process associated with degradation and very slow diffusion of the drug; and the erosion phase is a consequence of the polymer degradation due to hydrolysis of the ester bonds [24,29].

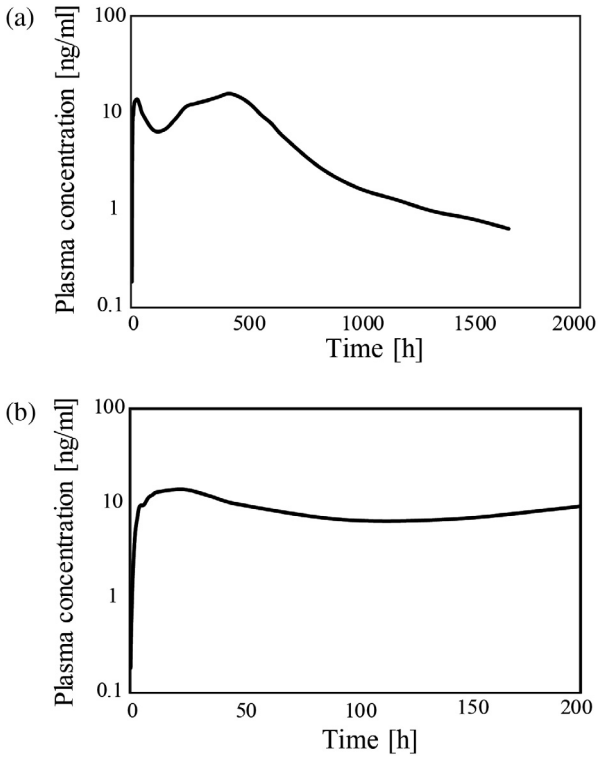

Fig. 2. (a) Peptide plasma concentrations/time profile after the i.m. injection of LR MS in log linear scale, and (b) magnification of (a) until 200 h.

3.3. Numerical deconvolution (DTC) of plasma concentrations for long-release dosage form

DTC method performs the convolution step simultaneously based on the convolution integral and prescribed function, which is also used for fitting of the input data. The numerical deconvolution method was selected as it is more flexible compared to the compartmental methods (*e.g.* it demands fewer assumptions as less modeling is required for UIR).

Knowing that studied PLGA LR MS released the peptide following a tri-phasic pattern and giving a sigmoidal shape curve, Weibull distribution (Eq. (3)) was used as prescribed function. It was already reported in the literature that fitting of drug release from PLGA microspheres demands modification of Weibull function [30]. As PLGA LR MS in general show burst release in the initial phase followed by an erosion phase, a double Weibull function is recommended in order to describe both processes in drug release. Double Weibull function is given by Eq. (6):

$$X_t = F_1[1-e^{-(t/\alpha_1)^{\beta_1}}] + F_2[1-e^{-(t/\alpha_2)^{\beta_2}}] \quad (6)$$

where: F_1 and F_2 are released fractions corresponding to burst and

Table 2
PK parameters after the i.m. injection of LR microspheres.

Parameter	$AUC_{0–48h}$ (ng h/ml)	AUC_{last} (ng h/ml)	AUC_{inf} (ng h/ml)	C_{max1} (ng/ml)	C_{max2} (ng/ml)	T_{max1} (h)	T_{max2} (h)
	549.3	9296.5	9890.2	13.8	16.1	24	432

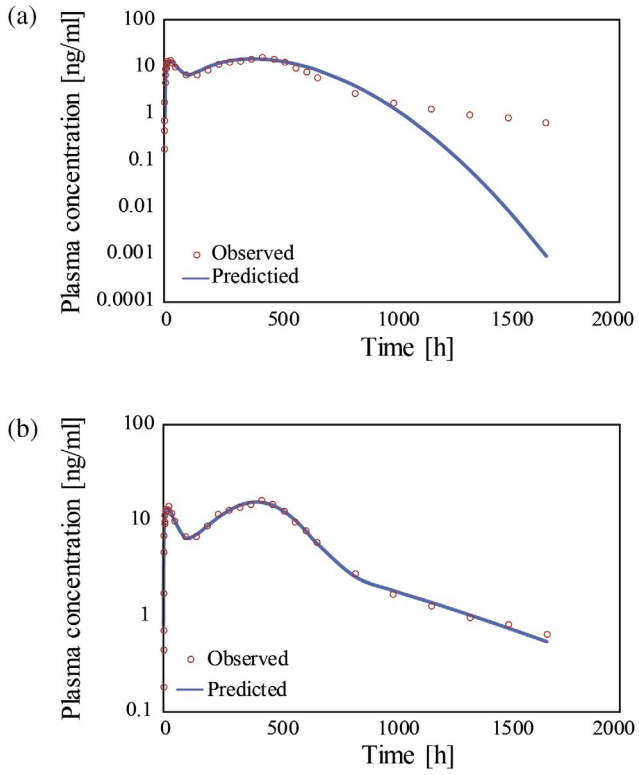

Fig. 3. Observed and predicted plasma concentrations by DTC method, log-linear scale: (a) double Weibull as prescribed function, (b) triple Weibull as prescribed function.

erosion phase, respectively (their sum is set to 1, as it is assumed that the complete amount of the injected peptide is bioavailable).

The *in vivo* input curve was generated by deconvolution based on double Weibull function. Same parameters were used for the convolution procedure which back calculates the plasma concentrations data, starting from the generated *in vivo* input. The advantage of this deconvolution method is that all calculations (deconvolution and convolution) are performed in one step. In such way, the calculated plasma concentrations were directly compared to the observed data and the goodness of fit by the prescribed function (Weibull) was estimated.

Fitted scale parameters were for α_1 35.2 h and for α_2 514.5 h, corresponding to burst and erosion peaks, respectively. Fractions assigned to each phase were F_1 0.1 (for burst phase) and F_2 0.9 (post-burst phase). Obtained SSQ and AIC values were 30.346 and 14.301, respectively.

Fig. 3a compares observed plasma concentrations with the calculated profile when double Weibull was used as prescribed function. It can be seen that the terminal part (840 h onwards) of the plasma concentrations/time curve was misestimated. This observation indicates that the double Weibull inadequately described all processes appearing *in vivo*.

In order to overcome this problem, a triple Weibull function was tested (Eq. (7)). Based on the literature research, the triple Weibull function was not used so far for fitting the drug release from PLGA microspheres. A new set of parameters was introduced (F_3, α_3, and β_3) to test if better prediction could be obtained. The sum of F_1, F_2, and F_3 was set to be equal to 1.

$$X_t = F_1[1-e^{-(t/\alpha_1)^{\beta_1}}] + F_2[1-e^{-(t/\alpha_2)^{\beta_2}}] + F_3[1-e^{-(t/\alpha_3)^{\beta_3}}] \quad (7)$$

The fitted fraction, shape, and scale parameters obtained by triple Weibull function are presented in Table 3. The SSQ (5.266) and AIC (-35.750) values indicated a significant improvement in fitting for triple Weibull. Fig. 3b shows the observed and estimated plasma concentration values when triple Weibull function was used as prescribed function in DTC method.

Table 3
Fraction (F), scale (α), and shape (β) parameters for triple Weibull function.

Weibull Parameter	F_1	α_1(h)	β_1	F_2	α_2 (h)	β_2	F_3	α_3 (h)	β_3
	0.1	29.6	1.2	0.4	460.6	3.2	0.5	695.0	1.2

Table 4
Percent prediction error (% PE) values between observed and predicted PK data for DTC method based on double and triple Weibull function.

Method - DTC	% PE				
Prescribed function	$AUC_{0\text{-}48h}$	AUC_{last}	AUC_{inf}	C_{max1}	C_{max2}
Double Weibull	1.4	9.8	15.2[a]	2.3	5.8
Triple Weibull	0.9	0.0	3.1	2.2	4.1

[a] Superior to 15% – unacceptable prediction according to the FDA guidance.

DTC using triple Weibull function gave significantly better prediction of plasma concentration values compared to double Weibull. This finding was confirmed by the decrease in SSQ, while lower AIC values exclude overfitting.

Compared to double Weibull function, triple Weibull gave very similar scale parameters for the burst (29.6 h) and erosion phase (460.6 h). The third part of the function fitted to the terminal phase of plasma concentrations/time curve (α_3 = 695 h), which contribution to the peptide release is 50% (F_3 = 0.5).

Table 4 summarizes % PE values obtained after performing DTC method using double and triple Weibull function. The % PE values were calculated as the absolute difference between observed PK parameters and parameters predicted from the deconvoluted *in vivo* input curve. AUC_{last} and AUC_{inf} were highly influenced by the choice of a prescribed function, as % PE values were much higher when double Weibull was used. For AUC_{inf}, the % PE was at the acceptance border (15%) using double Weibull [1,2]. While C_{max1} and C_{max2} were correctly estimated by both functions (double and triple Weibull), miss-prediction of AUC_{last} and AUC_{inf} reflects the incapacity of double Weibull function to fit correctly the terminal phase of the *in vivo* dissolution profile (as shown in Fig. 3a).

Some of possible reasons for the trend change in the last phase of drug release process from the studied PLGA-based LR MS are, for *e.g.*, change in the physiological environment triggered by an inflammatory reaction of the surrounding tissue, which might lead to formation of the fibrous capsule around the depot [31,32]; or change in the formulation structure due to the fact that microspheres are formulated using two PLGA polymers of different MW that might have different degradation kinetics.

3.4. Drug release mechanism from PLGA long-release microspheres

In order to investigate a possible reason for the phenomenon discussed above, the release mechanism from the tested PLGA-based LR MS was assessed. For this purpose, the *in vivo* input curve obtained after deconvolution by triple Weibull function was fitted to Peppas model. Fig. 4 shows the *in vivo* input profile (a) and the corresponding Peppas model (b).

Unexpectedly, Peppas model demonstrated the existence of 4 release phases. First phase (until 24 h) corresponded to burst release and was defined by the exponent n value of 1.14. Opposite to the currently existing hypothesis, which state that the burst release is mainly governed by the dissolution of immediately available drug substance on the microspheres' surface and diffusion through initially existing pores, obtained n value (> 0.85) is an indication of swelling controlled release

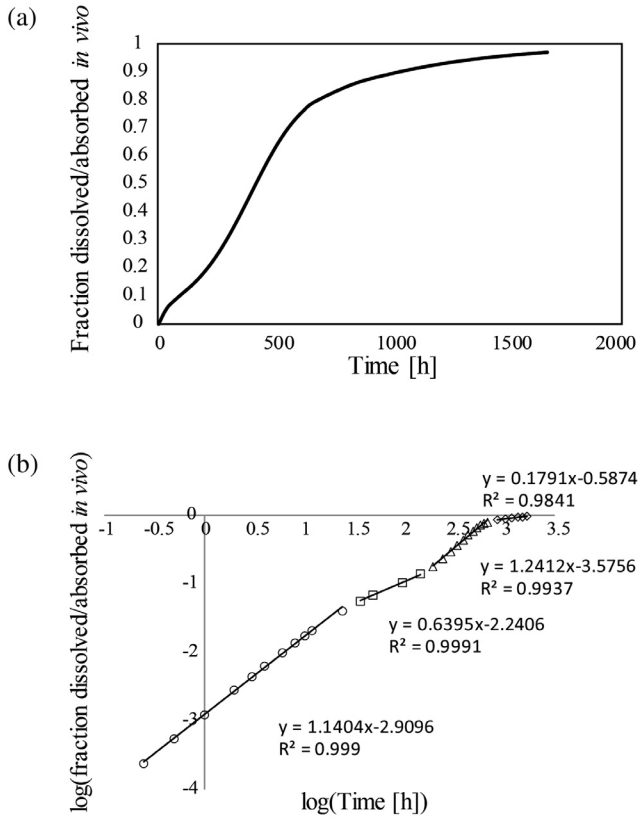

Fig. 4. (a) *In vivo* input profile obtained by DTC using triple Weibull function. (b) Fitted Peppas model for the same curve.

(Super Case-II). In the recent study of Gu et al. [33], the authors speculated that polymer swelling possibly contributes to drug release during the burst phase. Nevertheless, this finding represents the first evidence of the polymer swelling as a contributing factor on drug release during burst phase. The following phase (48 h to 144 h) corresponded to the lag and the exponent n had a value of 0.64, which is an indication of anomalous transport (mainly controlled by non-Fickian diffusion). The third phase (192 h to 672 h) was again characterized as Super case-II transport by the n value of 1.24. After the initial swelling and release process, the biologic fluids penetrate into the polymer network, leading to a depression in the glass transition temperature. Newly exposed polymer regions swell and become rubbery, and subsequently the softened polymer starts degrading (which is defined as an erosion phase of drug release) [34]. Finally, an additional, 4th phase could be discerned at the end of the drug release process (after 840 h) and was defined by the n value of 0.18. According to the original Peppas model, the exponent n can have only values greater than 0.43. Nevertheless, in case of the delivery systems where drug release occurs via diffusion through the polymeric network (as in the case of PLGA-based systems), the release exponent n is shifted towards smaller values. This is a consequence of a combined diffusion through a swollen matrix and through water-filled pores [19].

Even though the release mechanism from PLGA-based long-release delivery systems was mainly defined as tri-phasic release (burst, lag, and erosion) [24–27], Peppas model, fitted to the *in vivo* input curve obtained in human volunteers for the studied formulation, demonstrated the existence of the 4th phase. This phase was most probably a consequence of slow peptide diffusion through the matrix, created by fusion of the remaining swollen polymer fragments. In addition, the 4th release phase coincided with the trend change observed in plasma concentrations/time profile (Fig. 3a, 840–1008 h). This model demonstrated as well that the drug release during burst phase was not governed only by dissolution of immediately available peptide and its diffusion through existing pores, but also by polymer swelling after the absorption of interstitial fluids.

4. Conclusion

Based on the current findings, it can be seen that DTC method could successfully generate the *in vivo* input curve for very complex PLGA-based LR formulation. The use of Weibull as prescribed function was assessed and it was demonstrated that tri-phasic drug release profile, typical for PLGA-based formulations, demands triple Weibull function for correct estimation of the entire profile. The third set of Weibull parameters corresponded to terminal phase of drug release, as the release mechanism changed from erosion to diffusion controlled, leading to a change in the release rate. This phase in drug release (controlled by drug diffusion) was identified for the first time and confirmed by the Peppas model. The same model provided as well the evidence of polymer swelling contribution to burst release for the tested dosage form, which is in contrast with currently existing theories stating that burst release is mainly governed by the drug dissolution and diffusion.

Although the drug release from PLGA-based formulations was extensively investigated, this work represents the first study focusing on the *in vivo* input obtained in humans and providing the evidence of 4 different phases in the drug release.

Acknowledgements

This work was financially supported by Novartis Pharma AG, Switzerland.

References

[1] FDA guidance for industry extended release oral dosage forms: development, evaluation, and application of In Vitro/In vivo correlations U.S. Department of Health and Human Services Food and Drug Administration Center for Drug Evaluation and Research (CDER), 1997.
[2] European Medicines Agency, EMA/CPMP/EWP/280/96 Corr1, Guideline on the pharmacokinetic and clinical evaluation of modified release dosage forms, 2015.
[3] B. Mistry, N. Patel, M. Jamei, A. Rostami-Hodjegan, M.N. Martinez, Examining the use of a mechanistic model to generate an *In vivo/In vitro* correlation: Journey through a thought process, AAPS J. 18 (5) (2016).
[4] A. Margolskee, A.S. Darwich, A. Galetin, A. Rostami-Hodjegan, L. Aarons, Deconvolution and IVIVC: Exploring the role of rate-limiting conditions, AAPS J. 18 (2) (2015) 321–332.
[5] J.G. Wagner, E. Nelson, Percent absorbed time plots derived from blood level and/or urinary excretion data, J. Pharm. Sci. 52 (1963) 610–611.
[6] J.C.K. Loo, S. Riegelman, New method for calculating the intrinsic absorption rate of drugs, J. Pharm. Sci. 57 (1968) 918–928.
[7] D.J. Cutler, Numerical deconvolution by least squares: use of prescribed input functions, J. Pharmacokinet. Biopharm. 6 (3) (1978) 227–241.
[8] D.P. Vaughan, M. Dennis, Mathematical basis of point-area deconvolution method for determining *in vivo* input functions, J. Pharm. Sci. 67 (5) (1978) 663–665.
[9] F. Langenbucher, Handling of computational *in vitro/in vivo* correlation problems by Microsoft Excel: I. principles and some general algorithms, Eur. J. Pharm. Biopharm. 53 (2002) 1–7.
[10] F. Langenbucher, Handling of computational *in vitro/in vivo* correlation problems by Microsoft Excel: III. Convolution and deconvolution, Eur. J. Pharm. Biopharm. 56 (2003) 429–437.
[11] F. Langenbucher, Handling of computational *in vitro/in vivo* correlation problems by Microsoft Excel: II. Distribution functions and moments, Eur. J. Pharm. Biopharm. 55 (2003) 77–84.
[12] F. Langenbucher, Handling of computational *in vitro/in vivo* correlation problems by Microsoft Excel: IV. Generalized matrix analysis of linear compartment systems, Eur. J. Pharm. Biopharm. 59 (2005) 229–235.
[13] W. Weibull, A statistical distribution function of wide applicability, J. Appl. Mech. 18 (1951) 293–294.
[14] F. Langenbucher, Linearization of dissolution rate curves by the Weibull distribution, J. Pharm. Pharmacol. 24 (1972) 979–981.
[15] P. Costa, J.M. Sousa Lobo, Modeling and comparison of dissolution profiles, Eur. J. Pharm. Sci. 13 (2001) 123–133.
[16] S. Fredenberg, M. Wahlgren, M. Reslow, A. Axelsson, The mechanisms of drug release in poly(lactic-co-glycolic acid)-based drug delivery systems – A review, Int. J. Pharm. 415 (2011) 34–52.
[17] J.V. Andhariya, J. Shen, S. Choi, Y. Wang, Y. Zou, D.J. Burgess, Development of in vitro-in vivo correlation of parenteral naltrexone loaded polymeric microspheres, J. Control. Release. 255 (2017) 27–35.
[18] J.V. Andhariya, D.J. Burgess, Recent advances in testing of microsphere drug

delivery systems, Expert Opin. Drug Delivery 13 (4) (2016) 593–608.
[19] N.A. Peppas, Analysis of Fickian and non-Fickian drug release from polymers, Pharm Acta Helv. 60 (1985) 110–111.
[20] J.-M. Cardot, B.M. Davit, *In vitro-In vivo* correlation: Tricks and traps, AAPS J. 14 (3) (2012) 491–499.
[21] L.S. Lasdon, A.D. Waren, A. Jain, M. Ratner, Design and testing of a generalized reduced gradient code for nonlinear programming, ACM TOMS 4 (1) (1978) 34–50.
[22] P.L. Ritger, N.A. Peppas, A simple equation for description of solute release II. Fickian and anomalous release from swellable devices, J. Control. Release. 5 (1987) 37–42.
[23] E. Comets, F. Mentré, F. Nimmerfall, R. Kawai, I. Mueller, P. Marbach, Nonparamtetric analysis of the absorption profile of octreotide in rabbits from long-acting release formulation OncoLAR, J. Control. Release. 59 (1999) 197–205.
[24] B.S. Zolnik, P.E. Leary, D.J. Burgess, Elevated temperature accelerated release testing of PLGA microspheres, J. Control. Release. 112 (3) (2006) 293–300.
[25] B.S. Zolnik, D.J. Burgess, Effect of acidic pH on PLGA microsphere degradation and release, J. Control. Release. 122 (3) (2007) 338–344.
[26] B. Zolnik, D. Burgess, Evaluation of *in vivo-in vitro* release of dexamethasone from PLGA microspheres, J. Control. Release. 127 (2008) 137–145.
[27] H. Okada, One- and three-month release injectable microspheres of the LH-RH superagonist leuprorelin acetate, Adv. Drug. Deliv. Rev. 28 (1997) 43–70.
[28] M.J. Blanco-Prieto, K. Besseghir, O. Zerbe, D. Andris, P. Orsolini, F. Heimgartner, H.P. Merkle, B. Gander, *In vitro* and *in vivo* evaluation of a somatostatin analogue released from PLGA microspheres, J. Control. Release. 67 (2000) 19–28.
[29] J. Shen, D.J. Burgess, Accelerated *in vitro* release testing methods for extended-release parenteral dosage forms, J. Pharm. Pharmacol. 64 (7) (2012) 986–996.
[30] S. D'Souza, J.A. Faraj, P.P. DeLuca, A model-dependent approach to correlate accelerated with real-time release from biodegradable microspheres, AAPS PharmSciTech. 6 (4) (2005) 553–564.
[31] G.E. Visscher, R.L. Robison, H.V. Maulding, J.W. Fong, J.E. Pearson, G.J. Argentieri, Biodegradation of and tissue reaction to 50:50 poly(DL-lactide-co-glycolide) microcapsules, J. Biomed. Mat. Res. 19 (1985) 349–365.
[32] F.D. Anderson, D.F. Archer, S.M. Harman, R.J. Leonard, W.H. Wilborn, Tissue response to bioerodible, subcutaneous drug implants: A possible determination of drug absorption kinetics, Pharm. Res. 10 (1993) 369–380.
[33] B. Gu, X. Sun, F. Papadimitrakopoulos, D.J. Burgess, Seeing is believing, PLGA microsphere degradation revealed in PLGA microsphere/PVA hydrogel composites, J. Control. Release. 228 (2016) 170–178.
[34] C.S. Brazel, N.A. Peppas, Modeling of drug release from swellable polymers, Eur. J. Pharm. Biopharm. 49 (2000) 47–58.